European Journal of Nuclear Medicine and Molecular Imaging
https://doi.org/10.1007/s00259-021-05272-9

ORIGINAL ARTICLE

3D voxel-based dosimetry to predict contralateral hypertrophy and an adequate future liver remnant after lobar radioembolization

Fabiana Grisanti[1] · Elena Prieto[2] · Juan Fernando Bastidas[1] · Lidia Sancho[3] · Pablo Rodrigo[1] · Carmen Beorlegui[4] · Mercedes Iñarrairaegui[5] · José Ignacio Bilbao[6] · Bruno Sangro[5] · Macarena Rodríguez-Fraile[1]

Received: 21 September 2020 / Accepted: 17 February 2021

Abstract

Introduction Volume changes induced by selective internal radiation therapy (SIRT) may increase the possibility of tumor resection in patients with insufficient future liver remnant (FLR). The aim was to identify dosimetric and clinical parameters associated with contralateral hepatic hypertrophy after lobar/extended lobar SIRT with ^{90}Y-resin microspheres.

Materials and methods Patients underwent ^{90}Y PET/CT after lobar or extended lobar (right + segment IV) SIRT. ^{90}Y voxel dosimetry was retrospectively performed (PLANET Dose; DOSIsoft SA). Mean absorbed doses to tumoral/non-tumoral-treated volumes (NTL) and dose-volume histograms were extracted. Clinical variables were collected. Patients were stratified by FLR at baseline (T0-FLR): < 30% (would require hypertrophy) and ≥ 30%. Changes in volume of the treated, non-treated liver, and FLR were calculated at < 2 (T1), 2–5 (T2), and 6–12 months (T3) post-SIRT. Univariable and multivariable regression analyses were performed to identify predictors of atrophy, hypertrophy, and increase in FLR. The best cut-off value to predict an increase of FLR to ≥ 40% was defined using ROC analysis.

Results Fifty-six patients were studied; most had primary liver tumors (71.4%), 40.4% had cirrhosis, and 39.3% had been previously treated with chemotherapy. FLR in patients with T0-FLR < 30% increased progressively (T0: 25.2%; T1: 32.7%; T2: 38.1%; T3: 44.7%). No dosimetric parameter predicted atrophy. Both NTL-Dmean and NTL-V30 (fraction of NTL exposed to ≥ 30 Gy) were predictive of increase in FLR in patients with T0 FLR < 30%, the latter also in the total cohort of patients. Hypertrophy was not significantly associated with tumor dose or tumor size. When ≥ 49% of NTL received ≥ 30 Gy, FLR increased to ≥ 40% (accuracy: 76.4% in all patients and 80.95% in T0-FLR < 30% patients).

Conclusion NTL-Dmean and NTL exposed to ≥ 30 Gy (NTL-V30) were most significantly associated with increase in FLR (particularly among patients with T0-FLR < 30%). When half of NTL received ≥ 30 Gy, FLR increased to ≥ 40%, with higher accuracy among patients with T0-FLR < 30%.

Keywords Dosimetry · Yttrium-90 · SIRT · Radioembolization · Hypertrophy

Bruno Sangro and Macarena Rodríguez-Fraile contributed equally to this work.

This article is part of the Topical Collection on Dosimetry

✉ Fabiana Grisanti
fabianagrisanti@gmail.com

[1] Department of Nuclear Medicine, Clínica Universidad de Navarra, Pamplona, Spain

[2] Department of Medical Physics, Clínica Universidad de Navarra, Pamplona, Spain

[3] Department of Nuclear Medicine, Clínica Universidad de Navarra, Madrid, Spain

[4] Department of Health, Government of Navarre, Pamplona, Spain

[5] Liver Unit, Clínica Universidad de Navarra-IDISNA and CIBEREHD, Pamplona, Spain

[6] Department of Radiology, Clínica Universidad de Navarra, Pamplona, Spain

Published online: 05 March 2021

Introduction

Selective internal radiation therapy (SIRT), also termed radioembolization, is an established treatment for primary and secondary unresectable hepatic malignancies [1], in which Yttrium-90 (^{90}Y)-loaded resin microspheres are injected in the arterial vasculature of the liver. While most microspheres get embedded into the tumor vasculature due to its mainly arterial irrigation, those beads that are deployed in the non-cancerous liver parenchyma also deliver radiation to this tissue compartment. Such liver absorbed radiation may in turn result in clinical [2] or subclinical [3] liver damage. Significant liver atrophy following whole-liver SIRT may induce clinical decompensation [2].

Lobar SIRT may induce volumetric changes in the liver, with atrophy of the treated volume and hypertrophy of the spared liver volume [4–12]. The mechanism of this "atrophy-hypertrophy complex" is not fully understood. The fact that contralateral hypertrophy is consistently associated with ipsilateral atrophy suggests that it may be a compensatory mechanism [13]. The importance of such compensatory hypertrophy is that it can allow tumor resection in patients in whom the future liver remnant (FLR) is insufficient before SIRT [12]. Indeed, contralateral hypertrophy can be one of the aims of SIRT in certain clinical scenarios. In patients with good liver function, a FLR of at least 25–30% is considered sufficient to prevent liver failure [14]. However, in patients with cirrhosis, up to 40% must be preserved [15, 16].

Recently, there is a great interest in the influence of dosimetric and biologic effects of radionuclide therapies, while quantitative imaging is becoming a significant part of the treatment planning workflow [17]. ^{99m}Tc-labeled macroaggregates of albumin (^{99m}Tc-MAA) scintigraphy is part of the treatment planning for SIRT, and dosimetric approaches to calculate the prescribed activity have been designed to enhance tumor dose and reduce toxicity in an attempt to improve patient outcomes [2, 18–22]. Few dosimetric studies have attempted to predict contralateral liver hypertrophy after lobar SIRT, based on pre-SIRT ^{99m}Tc-MAA findings [23]. However, simulation studies with ^{99m}Tc-MAA before SIRT only depict what the microsphere biodistribution will likely be after injection. The benefit of post-SIRT ^{90}Y PET/CT is that it provides an accurate estimation of the actual microsphere biodistribution [20].

The goal of this study is to evaluate ^{90}Y dosimetric and clinical parameters that predict atrophy of the treated lobe (as a surrogate for subclinical liver damage induced by radiation) and hypertrophy of the contralateral lobe (as a potential primary or secondary treatment aim) after lobar or extended lobar SIRT with ^{90}Y-loaded resin microspheres. To our knowledge, this is the first study to investigate the relation between dosimetric findings on ^{90}Y PET/CT (after SIRT with ^{90}Y-loaded resin microspheres) and both ipsilateral atrophy and contralateral hypertrophy.

Material and methods

Patient cohort

This retrospective study included all patients with primary or secondary hepatic tumors treated with ^{90}Y-loaded resin microspheres (SIR-Spheres, Sirtex Medical Europe GmbH) at our institution between December 2011 and December 2019 in whom (i) lobar (right or left) or lobar extended (right lobe plus segment IV) SIRT was performed; (ii) ^{90}Y PET/CT (^{90}Y PET) was obtained; and (iii) one or more cross-sectional imaging studies were completed at least within 2 months after SIRT. Imaging studies at follow-up were scheduled by clinicians at different points in time, depending on tumor type, treatment aim, and other factors. For the purpose of this study, they were grouped in three time intervals, namely 0–2 months (T1), 2–6 months (T2), and at 6–12 months (T3) after SIRT. In patients that received a second SIRT treatment or were submitted to any hepatic intervention after SIRT, including hepatectomy or biliary drainage, their subsequent images were excluded from analysis.

The current general inclusion criteria for SIRT in our center are (i) an unequivocal diagnosis of unresectable cancer with liver-only or liver-dominant tumor burden, (ii) a life expectancy of > 3 months, (iii) an Eastern Cooperative Oncology Group (ECOG) performance status of 0–1, (iv) a lung shunt fraction (LSF) ≤ 20%, and (v) adequate pulmonary, hematological, hepatic, and renal function.

As in many patients SIRT was not applied to induce hypertrophy of the FLR as a primary aim (i.e., palliative or curative intent, as salvage therapy), FLR was not necessarily insufficient. However, for analytical purposes, the patients were divided into two groups according to baseline FLR: < 30% (would require hypertrophy to prevent postoperative liver failure [14]) and ≥ 30% (would not require hypertrophy to prevent postoperative liver failure unless cirrhotic [15, 16]). An FLR ≥ 40% was considered adequate for both patients with and without cirrhosis [15, 16]).

The institutional Ethics Committee approved the protocol (212/2019) for this retrospective study and waived the need for patient informed consent. The study was performed in accordance with the ethical standards laid down in the 1964 Declaration of Helsinki and all subsequent revisions.

Pre-treatment and treatment

Pre-treatment investigations included CT or MRI scans, blood cell count, and serum biochemistry. Regarding baseline imaging scans (T0), 39 patients (69.6%) had a CT and 17 patients

(30.4%) had an MRI. Our protocol for SIRT has already been published [24]. In summary, images were carefully assessed before angiographic mapping of the abdominal and hepatic arteries. Planar scans of the lung and liver area in anterior and posterior views were acquired after injection of ^{99m}Tc-MAA into selected arterial branches followed by SPECT/CT. They were used for (a) calculation of LSF, (b) calculation of tumor/non-tumor (T/N) ratio, and (c) detection of any non-target infused liver volume and the unintentional delivery of radioactive particles to organs outside the liver. For lobar or lobar extended SIRT (all the patients in this study), the prescribed ^{90}Y activity was calculated using the partition model, taking into account LSF, T/N ratio, target tumor volume, and target hepatic volume from the ^{99m}Tc-MAA study, considering optimal absorbed doses by tumoral and non-tumoral volumes [24]. SIR-Spheres were injected within 15 days of the ^{99m}Tc-MAA scan. In all cases, a same-day calibration 3 GBq vial was used (44 ± 2.6 million spheres per vial) [25].

PET ^{90}Y imaging

The day after SIRT (14–17 h after treatment), ^{90}Y PET imaging was performed to evaluate extrahepatic activity deposition and intrahepatic microsphere distribution, and to permit voxel dosimetry quantification. ^{90}Y PET images were acquired on a Siemens Biograph mCT TrueV scanner (Siemens Medical Solutions, Hoffman States, IL, USA). The ^{90}Y PET acquisition duration was 30 min (10 min per bed position) where complete chest and abdomen areas were included. ^{90}Y PET images were reconstructed on 200 × 200 matrix using an iterative method (OSEM) including algorithms for PSF (point spread function) recovery and TOF (time of flight) calculation (1 iteration and 21 subsets), including a Gaussian post-reconstruction filter (5 mm) with CT-based correction, published elsewhere [26]. CT images were acquired in a spiral mode (pitch 1.2, 120 kVp, and care dose 4D).

Dosimetric analysis

Retrospective ^{90}Y PET-based voxel dosimetry was performed using a dedicated treatment planning system (PLANET Dose; DOSIsoft SA). The image files for T0 and follow-up studies were imported, and an anatomic outline of the total treated volume (right lobe, right lobe plus segment IV, or left lobe), and non-treated volume (contralateral, spared volume) were made on the axial plane on portal phase contrast-enhanced CT, MR images, or on the CT of PET/CT by a nuclear medicine physician. The total liver volume was acquired through volumetric Boolean sum. Within the treated volume, the delineation of the tumor was also made on anatomic images. Rigid registration was performed, and contours were propagated to the ^{90}Y PET, and adjusted manually as needed in order to correct millimetric errors in registration. The non-tumoral target liver (NTL) volume was defined by excluding the tumor volume from the target liver.

A 3-dimensional dose map was calculated using a kernel convolution algorithm at the voxel level. The mean dose (Dmean) to the total target liver, NTL, and tumor volumes was studied, as well as other metrics extracted from dose-volume histograms (DVH): the minimum dose to 20%, 50%, 70%, 90% 95%, and 98% of the NTL or tumor volume and the percentage of the volume receiving at least 30, 40, 50, 70, 100, and 120 Gy.

For ^{99m}Tc-MAA, the voxel dosimetry analysis was not performed. Mean doses estimated to the tumor and NTL were obtained by formula derived from the ^{99m}Tc-MAA study (bidimensional T/N ratio and LSF), and from CT/MRI (tumor volume and non-tumor volume) and used for activity calculation.

Follow-up evaluation

Atrophy and hypertrophy were assessed as absolute (ml) and relative (%) changes between volumes at T0 (corresponding to the most recent CT or MR images prior to SIRT), and at T1, T2, and T3. The FLR was defined as the ratio between the volume of non-treated liver and total liver volume. The FLR was calculated at T0, T1, T2, and T3. Maximal hypertrophy (MHT) and its time of occurrence were also calculated.

Clinical and laboratory data were retrospectively collected from each time point. Specific SIRT complications that were searched in medical records included (a) post-radioembolization syndrome (PRS), defined as the occurrence of self-limited fever, fatigue, abdominal pain, nausea, vomiting, or anorexia [27]; (b) radioembolization-induced liver disease (REILD) [2]; and (c) non-target delivery of radiation to lung or gastrointestinal tract (pneumonitis, gastrointestinal ulceration, cholecystitis). Tumor response was assessed using Response Evaluation Criteria in Solid Tumors version 1.0 [28]. It was evaluated until 9 months after SIRT or until a surgical, systemic, or new local treatment in the same lobe was used. Patients who received hepatectomy post-radioembolization were also recorded.

Statistical analysis

Descriptive statistics were produced for quantitative variables and frequency and percentage for categorical variables. Univariate regression analysis was performed in the entire cohort, and in patients with FLR < 30 and ≥ 30%. Variables considered were dosimetric (injected, mean dose to tumor and NTL according to ^{99m}Tc-MAA dosimetry by formula, and 3D voxel based in 90Y PET parameters, i.e., mean dose and DVH values to the tumor and NTL), clinical (age, sex, presence of cirrhosis, prior chemotherapy, prior TACE, treatment-naïve status, chemotherapy post-SIRT, primary vs. secondary tumors, unifocal or multifocal tumor, SIRT injection approach),

and volumetric (target and non-target liver volume, tumor volume, tumors larger or smaller than 100 ml, and tumor to target liver volume ratio).

Variables associated with hypertrophy or increase in FLR in the total cohort with a p value < 0.2 were further considered; multivariate analyses were performed to identify the best predictors of atrophy, hypertrophy, and increase in FLR in patients with FLR < 30 and ≥ 30%.

Receiver operator characteristic (ROC) curves were used to identify optimal cut-off points for prediction of increase in FLR to ≥ 30% and ≥ 40% (the latter, an adequate FLR for surgery even in cirrhotic patients [29]). Sensitivity, specificity, positive predictive value (PPV), negative predictive value (NPV), positive likelihood ratio (LR+), negative likelihood ratio (LR−), and accuracy of predictors were calculated. Different dosimetric and volumetric parameters were correlated with NTL atrophy and contralateral hypertrophy through Spearman's Rho. Volume changes in the total target liver, in the NTL, as well as in the non-treated lobe (in ml and percentage change) between different time periods were studied using the Wilcoxon test for related samples. Atrophy and hypertrophy in cirrhotic and non-cirrhotic patients, as well as in patients with other clinical variables, were compared using the Mann-Whitney U test.

The correlation between NTL atrophy and contralateral hypertrophy was also determined with Spearman's Rho. The concordance between these last two variables was measured by means of Lin's concordance coefficient. Stata version 12.0 (Stata Corporation, College Station, Texas, USA) was used for statistical analysis. Values of $p < 0.05$ were considered statistically significant.

Results

Patients

Fifty-six patients met patient selection criteria and their general characteristics are summarized in Table 1. Most patients had primary liver tumors (71.4%) and 40.4% had cirrhosis. Liver and hematological functions were basically preserved. During follow-up, 51 patients had imaging studies at T1, 45 at T2, and 23 at T3. Median time from SIRT was 1.79 months (IQR: 0.63) for T1, 4.12 months (IQR: 1.45) for T2, and 8.97 months (IQR: 2.53) for T3. Dosimetric parameters are summarized in Table 2.

Atrophy and hypertrophy

There was a progressive decrease in the volume of the treated segments (Fig. 1, Table 3) that was statistically significant in each time period compared to the previous one. These results remained consistent in patients in whom the right hemi-liver or right + segment IV were treated. However, in patients with left lobar SIRT, the volume of the treated liver decreased significantly only starting from T2 ($p = 0.011$). A progressive increase in the volume of the non-treated liver was observed (see Table 3 and Fig. 1). This was statistically significant between T0 and T1 ($p < 0.001$), and between T1 and T2 ($p = 0.002$), but not between T2 and T3 ($p = 0.178$).

Total liver volume progressively decreased, although differences were not statistically significant in any time period. Compared to T0 (1919.7 ± 671.8 ml), total liver volume decreased at T1 (1891.2 ± 725.5 ml; $p = 0.290$), to T2 (1791 ± 639.8 ml; $p = 0.052$), and T3 (1567.7 ± 522.9 ml; $p = 0.059$), because hypertrophy of the non-treated liver partially compensated for the atrophy of the treated segments. Maximal hypertrophy was 36.40 ± 40.64% and occurred mostly at T2 (4.47 ± 2.82 months).

Increase in FLR, changes in liver function, and outcomes

FLR progressively increased in all patients, as well as in patients with FLR < 30% and ≥ 30% at T0 (see Table 3).

A clinically irrelevant but statistically significant increase in total bilirubin was observed from T0 (0.67 ± 0.38 mg/ml) to T1 (1.02 ± 0.93 mg/ml; $p < 0.001$), T2 (1.38 ± 1.88 mg/ml; $p < 0.001$), and T3 (1.29 ± 1.41 mg/ml; $p = 0.006$). No significant changes in synthetic liver function (prothrombin time, INR, and albumin) were seen.

Clinically, post-radioembolization syndrome occurred in ten patients (17.8%). No patients had REILD or pneumonitis. Two patients with gastric or duodenal uptake detected on ^{90}Y PET developed a gastric and a duodenal ulcer respectively, diagnosed 2 to 3 months after SIRT, both treated symptomatically and one requiring endoscopic treatment. Six patients were lost at follow-up, one deceased, and five due to continuing follow-up at another hospital center (with available imaging but not clinical data). Out of the remaining 50 patients, 10 patients maintained stable disease, 15 obtained partial response, and 4 obtained complete response. After radioembolization, 11 patients (19.6%) underwent hepatectomy. Progressive disease was observed in 21 patients (6 ipsilateral, 11 contralateral, and 4 bilateral).

Prediction of contralateral hypertrophy and increase in FLR

Analyses focused on hypertrophy between T0 and T2, when maximal hypertrophy was mostly found, given that there were no significant changes in hypertrophy between T2 and T3 and the number of patients with available imaging studies was larger in T2 than in T3.

Univariable regression NTL-Dmean, obtained from 99mTc-MAA and 90Y PET, was significantly associated with contralateral hypertrophy among patients with T0 FLR < 30%

Table 1 General characteristics of patients in the present series ($n = 56$)

Characteristics	*N*	(%)
Type of tumor		
•Primary liver tumors	40	71.4
Hepatocarcinoma	29	51.8
Cholangiocarcinoma	9	16.1
Mixed hepatocarcinoma/cholangiocarcinoma	2	3.6
•Liver metastases	16	28.5
Colorectal cancer	7	12.5
Neuroendocrine tumors	4	7.1
Other	5	8.9
Prior therapies		
Hepatic resection	10	17.8
Radiofrequency ablation	11	19.6
Transarterial chemoembolization (TACE)	12	21.4
Prior chemotherapy	22	39.3
Antiangiogenic drugs	6	10.7
Disease distribution		
Uninodular	16	28.6
Multinodular	40	71.4
Tumor burden < 100 ml median: 31.6, IQR 50.5 ml	28	50
Tumor burden ≥ 100 ml median: 332.2, IQR 400.7 ml[1]	28	50
Cirrhosis	19	40.4
Albumin-bilirubin (ALBI) grade		
Grade 1	5	8.9
Grade 2	51	91.1
SIRT approach		
Right lobar	38	67.9
Extended right lobar (right + segment IV)	6	10.7
Left lobar	12	21.4
Laboratory data	Median	IQR
AST, UI/l	31	22
ALT, U/I	27	24
Alkaline phosphatase, UI/l	109	73
γ-GTP, UI/l	115.5	183
Total bilirubin, mg/dl	0.55	0.43
Albumin, g/dl	3.78	0.665
ALBI score	− 2.62	0.35
Platelets, 109/l	177	125
International normalized ratio (INR)	1.1	1

[1] Largest tumor size: 1495 ml (treated lobe: 2300 ml)

(99mTc-MAA: $p = 0.024$; 90Y PET: $p = 0.009$). Similarly, NTL-Dmean obtained from 90Y PET was a significant predictor of increase in FLR ($p = 0.001$) among patients with T0 FLR < 30%. NTL-V30 was a significant predictor of increase in FLR in the total cohort ($p = 0.033$). Likewise, it was a predictor of both contralateral hypertrophy ($p = 0.007$) and increase in FLR ($p = 0.004$) just among patients with T0 FLR < 30%. NTL-D95 and NTL-D98 ($p = 0.026$ and 0.015 respectively) were also significantly associated with increase in FLR in the total cohort of patients, but not according to T0 FLR < 30% or ≥ 30%.

Injected activity was not a statistically significant predictor of hypertrophy. Hypertrophy and increase in FLR were not significantly associated with any dosimetric variables related to tumor dose (neither in 99mTc-MAA nor in 90Y PET) or tumor size. Dosimetric, clinical, and baseline volumetric variables associated with hypertrophy and increase in FLR are further described in Supplementary Table 1.

Table 2 Dosimetric parameters

Variables	Values: Mean ± SD
Injected activity	1.56±0.67 GBq
Total target liver-Dmean in Y90-PET	58.99±24.04 Gy
NTL-Dmean predicted from 99mTc-MAA	59.45±35.42 Gy
NTL-Dmean in Y90-PET	50.73±24.69 Gy
NTL-V30	58.82±21.95%
NTL-D95	7.55±7.65 Gy
Tumor-Dmean predicted from 99mTc-MAA	122.51±64.23 Gy
Tumor-Dmean in Y90-PET	117.90±78.57 Gy

SD standard deviation, *Dmean* mean dose (Gy), *V30* percent of treated volume that receives at least 30 Gy, *NTL* non-tumoral target liver; *D95* dose that 95% of the treated volume receives

Among clinical variables, the presence of a secondary tumor ($p = 0.023$) and prior chemotherapy ($p = 0.027$) were significantly associated with hypertrophy and increase in FLR. The volume of the non-target liver was also significantly associated with hypertrophy and increase in FLR in the total cohort of patients.

Sex, abnormal platelet count, prothrombin time or serum transaminases, prior TACE, and chemotherapy post-SIRT were also not significantly associated with hypertrophy or increase in FLR. Moreover, the presence of cirrhosis, total bilirubin at T0, and SIRT approach obtained a significance of $p < 0.2$ but did not reach statistical significance.

Multivariable regression In patients with the smaller FLR, NTL-V30 was the most significant predictor of an increase in FLR (adjusted R^2: 0.609; see Fig. 2, and Supplementary Table 2). It also predicted the degree of hypertrophy (adjusted R^2: 0.336) at T2. In these patients, the correlation between NTL-V30 and increase in FLR at T2 was 0.608 with Spearman's Rho.

In contrast, in patients with the larger FLR ≥ 30% at T0, NTL-V30 was not significantly associated with hypertrophy or increase in FLR (R^2: 0.02, $p = 0.508$; see Fig. 2). In these patients, the volume of the non-treated liver at T0 and total injected activity were independent predictors of an increase in FLR (R^2: 0.34; adjusted R^2: 0.28; Supplementary Table 3).

ROC analysis ROC analysis was performed with dosimetric parameters to identify cut-off points to predict increase in FLR, described in Table 4. A cut-off of ≥49% in the fractional non-tumor volume that receives 30 Gy (NTL-V30) obtained the highest accuracy to predict increase in FLR, and with higher accuracy in patients with T0 FLR < 30%, with a sensitivity, specificity, PPV, NPV, and accuracy of 80.00%, 81.82%, 80.00%, 81.82%, and 80.95% (AUC: 0.809) respectively (Fig. 3).

Prediction of atrophy of the treated hemi-liver and correlation with hypertrophy of the non-treated liver

No individual parameter of the dose/volume histogram was significantly associated with atrophy of the treated segments. Variables at T0 significantly associated with atrophy at T2 in the total cohort of patients were total bilirubin ($p = 0.192$) and the volume of the non-treated liver ($p = 0.014$), although these associations were not robust in multivariable analysis (see Supplementary Table 4).

A weak correlation was observed between atrophy of the treated segments and hypertrophy of the non-treated liver (Spearman's Rho, − 0.213 in T1, 0.362 in T2, and 0.351 in T3). Concordance between both variables showed a Lin coefficient of 0.308.

Discussion

In this study, clinical and dosimetric parameters were evaluated in ^{90}Y PET following lobar SIRT with ^{90}Y-loaded resin microspheres, in order to identify variables associated with contralateral hypertrophy in the non-treated liver after SIRT (as a potential primary or secondary treatment aim) or with atrophy of the treated lobe (as a surrogate for subclinical liver damage induced by radiation).

Dosimetric analysis revealed that several variables related to the dose absorbed by the NTL were the most significant predictors of contralateral hypertrophy or increase in FLR. In the univariate analysis, predictors of both were NTL-Dmean in PET and NTL-V30, the latter in the entire cohort and in patients with T0 FLR < 30%, not so in patients with FLR ≥ 30%. To our knowledge, this is the first demonstration of a correlation between a ^{90}Y PET dosimetric parameter and the degree of hypertrophy with resin microspheres. An inadequate FLR is one of the most common reasons for precluding otherwise suitable patients from potentially curative liver resection. A FLR of at least 30% is required for patients with preserved liver function, and at least 40% is required for cirrhotic patients [29]. Furthermore, an increase in FLR to ≥ 40% was

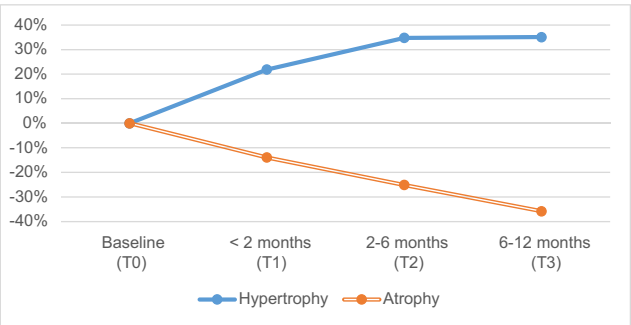

Fig. 1 Changes in volume (%) of the treated (atrophy) and non-treated liver (hypertrophy) after radioembolization

Table 3 Atrophy, hypertrophy, and changes in the future liver remnant at baseline and during follow-up

	T0	T1	T2	T3
Atrophy of the treated hemi-liver				
Change in %		− 13.9±13.4	− 25.1±18.7	− 35.8±17.9
Volume in ml	1183.1 ± 571.3	1037.9±519.7	904.9±522.1	679.9±391.7
p value*		< 0.001	< 0.001	0.007
Hypertrophy of the non-treated liver				
Change in %	762 ± 379	+ 21.9±29.8	+ 34.8±54.4	+ 35.1±35.2
Volume in ml		882.5±514	906.2±399.8	959.1±356
p value*		< 0.001	0.002	0.178
Future liver remnant (FLR; %)				
All patients	40.4 ± 17	46.1±17	51.9±17.3	64.5±16.5
p value*		< 0.001	< 0.001	0.002
FLR < 30% at T0	25.2 ± 4.4	32.7±9.4	38.1±11.6	44.7±12.1
p value*		< 0.001	< 0.001	0.225
FLR ≥30% at T0	50.3 ± 14.6	55.4±14.8	62±13.3	70±13.1
p value*		< 0.001	< 0.001	0.004

FLR future liver remnant, *T0* baseline, *T1* 0–2 months after SIRT, *T2* 2–6 months after SIRT, *T3* 6–12 months after SIRT

Mean ± standard deviation (SD). Positive and negative changes are indicated with (+) and (−) respectively

*Compared to previous time period

predicted by a NTL-V30 of 49%, with a sensitivity, specificity, and accuracy of 78.6%, 69.2%, and 76.4%.

An important finding of our study is the influence of the baseline volume of the non-treated liver. It was negatively associated with contralateral hypertrophy and with an increase in FLR. In other words and not surprisingly, larger contralateral lobes achieved a lower degree of hypertrophy than smaller ones. This may be partially attributed to larger contralateral lobes already hypertrophied due to cirrhosis, consistent with Goebel et al.'s [30] finding that the baseline relative left liver volume (defined as left liver volume/total liver volume) was significantly higher in patients with cirrhosis than in patients without cirrhosis. As importantly, these findings suggest that those local factors that trigger hypertrophy are not induced or are not as effective in large FLRs. In our study, cirrhosis approached, but did not reach statistical significance.

Palard et al. [23] evaluated dosimetric parameters associated with contralateral hypertrophy in patients treated with ^{90}Y-loaded glass microspheres. However, they studied dosimetric parameters from ^{99m}Tc-MAA and not from ^{90}Y PET, which demonstrates the true distribution of injected activity. In our study, we compared NTL-Dmean of ^{99m}Tc-MAA obtained by formula with 3D voxel-based dosimetry in ^{90}Y PET. Congruent with our study, they found that NTL-Dmean with ^{99m}Tc-MAA was associated with MHT > 10%, while Tumor-Dmean and injected activity as continuous variables were not. Our study focused on the increase in FLR instead of MHT > 10% because we believe that the former is more clinically relevant. In our study, NTL-Dmean in ^{99m}Tc-MAA and ^{90}Y PET were statistically significant in the univariable analysis only in patients with FLR < 30.

Currently, there are three types of microspheres (TheraSphere, SIR-Spheres, and QuiremSpheres) and each of them has different properties [31]. In patients treated with SIR-Spheres, the number of particles used is higher than patients treated with TheraSphere (20–40 million vs. 5 million) producing a more relative embolic effect, with lower specific

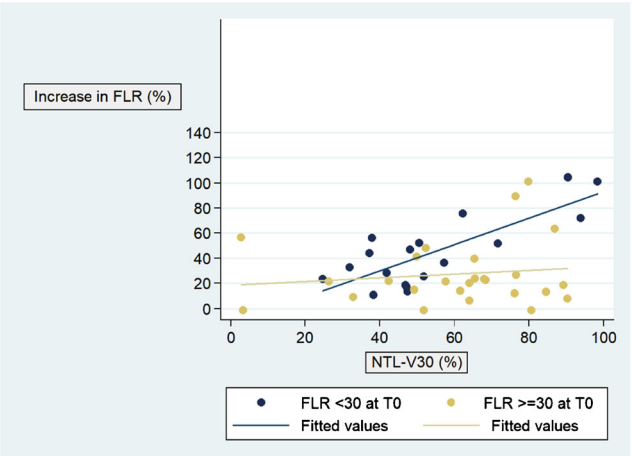

Fig. 2 *FLR:* the ratio between the volume of non-treated liver and total liver volume in percent; *NTL-V30*: percent of the non-treated volume that receives at least 30 Gy; *T0:* baseline; *T2:* 2–6 months. Scatter plot of percent increase in FLR in T2 according to patients with FLR < 30% and ≥ 30% at T0. NTL-V30 was associated with increase in FLR in patients with the lower FLR < 30% at T0 (adjusted R^2: 0.609), but not in patients with the higher FLR ≥ 30% at T0 (adjusted R^2: 0.336)

Table 4 ROC analysis of dosimetric parameters

Dosimetric parameter	Cut-off	Endpoint	Sensitivity	Specificity	Accuracy	LR+	LR−	AUC
NTL-Dmean	≥ 40.17 Gy[1]	FLR≥30%	60.8%	80%	62.5%	3.039	0.490	0.765
NTL-V30	≥ 48.03%[1]		74.5%	80%	75%	3.726	0.319	0.796
NTL-D95	5.98 Gy[1]		51%	80%	53.6%	2.549	0.618	0.608
NTL-D98	3.16 Gy[1]		47.1%	80%	50%	2.353	0.662	0.577
NTL-Dmean	≥ 56.48 Gy[1]	FLR ≥40%	48.8%	92.3%	58.9%	6.349	0.554	0.680
NTL-V30	≥ 49.07%[2]		79.1%	69.2%	76.8%	2.570	0.302	0.734
NTL-D95	≥ 7.39 Gy[1]		51.2%	92.3%	60.7%	6.651	0.529	0.667
NTL-D98	≥ 3.98 Gy[1]		41.9%	92.3%	53.6%	5.442	0.630	0.629

NTL non-tumoral target liver, *Dmean* mean dose (Gy), *V30* percent of treated volume that receives at least 30 Gy, *D95* dose that 95% of the treated volume receives, *D98* dose that 98% of the treated volume receives, *LR+* positive likelihood ratio, *LR−* negative likelihood ratio, *AUC* area under the curve

[1] With the highest LR+

[2] With the highest accuracy

activity per microsphere (20–70 vs. 4354 Bq per microsphere). QuiremSpheres have an intermediate position in terms of number of particles (20 millions), specific activity (240–375 Bq/microsphere), and embolic effect [31]. As described by Pasciak et al. [32], differences in microsphere-number density may have an effect on microscopic tumor absorbed dose inhomogeneity. Our study was carried out with SIR-Spheres which present the highest number of particles injected, and it seems that the results obtained in our study may not be extrapolated to the other two types of microspheres, with different absorbed dose distribution.

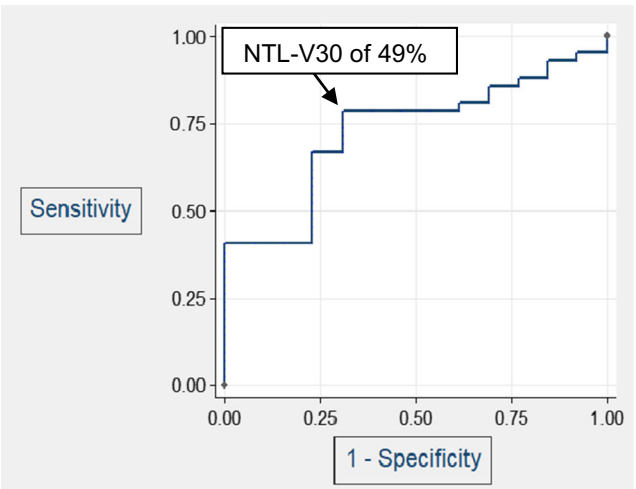

Fig. 3 *ROC*, receiver operator characteristic; *NTL-V30*, percent of the non-treated volume that receives at least 30 Gy; *PPV*, positive predictive value; *NPV*, negative predictive value; *AUC*, area under the curve. ROC curve with the highest accuracy to predict an increase in FLR to ≥ 40% with a cut-off of 49% of NTL-V30. This was performed with all patients. The sensitivity, specificity, PPV, NPV, and accuracy were 78.57%, 69.23%, 89.19%, 50.00%, and 76.36% respectively. The AUC was 0.727

It should be noted that all our patients were treated according to the partition model, standard at our institution for lobar and selective treatments [31], and none of them developed REILD. This result supports the use of this multi-compartment method as a safe method of activity planning.

Volume changes in our study are consistent with those reported in the literature. In a systematic review of contralateral hypertrophy after unilobar SIRT [12], contralateral liver hypertrophy ranged from 26 to 47% in a period of time between 44 days and 9 months. In our series, the mean increase in volume of the non-treated liver at T2 was 34%. Another study [7] similarly found an increase in FLR of 36% at both 3–6 and 6–9 months. In a previous report from our group, the degree of hypertrophy was higher (45% at 26 weeks), probably due to the less frequent use of the partition model in earlier times [13].

In our study, neither tumor size (as a continuous variable or as smaller or larger than 100 ml) nor tumor dose (mean, maximum, or other DVH results) was significantly associated with contralateral hypertrophy. The lower degree of hypertrophy after left lobar SIRT compared to right or extended right lobar SIRT, and among cirrhotic patients has been reported elsewhere [9, 13], though these factors did not reach significance in the present study. Clinical factors associated with hypertrophy were the presence of secondary tumors and prior chemotherapy.

Hepatobiliary scintigraphy (HBS) is an emerging nuclear imaging technique to quantitatively assess global and regional liver function [33]. The main indication for HBS is to assess the FLR function in patients scheduled to undergo hemi-hepatectomy, to predict the risk of post-hepatectomy liver failure, particularly in patients with impaired liver function due to cirrhosis or after chemotherapy [33]. In the work-up for radioembolization, patients may be further screened by HBS given that analysis of clinical and laboratory parameters may

not be sufficient. HBS may improve patient selection and treatment planning for radioembolization, in order to evaluate if the liver function of the non-treated lobe is sufficient to compensate for radiation damage in the treated part of the liver [34]. Furthermore, it may be useful to assess how well the magnitude of hypertrophy correlates with changes in liver function after radioembolization. Larger studies should explain the numeric relation between the absorbed dose to the functional liver parenchyma and the decline in liver function after radioembolization [34].

A relevant observation is the failure to identify dosimetric parameters related to liver atrophy. The initial assumption was that a higher absorbed dose would result in a higher degree of atrophy, but the results in this study do not support this hypothesis. This surprising finding suggests that the distribution of the radioactive beads or the different sensitivity of different areas of the liver acinus may play a role [35], and certainly deserves further research.

There are several limitations in this study. Firstly, it is a retrospective study with a small sample size, which limits the predictive power of the results. On the other hand, SIRT was not always performed with the primary intention to hypertrophy the non-treated liver as a bridge to surgical resection, in patients in whom a low FLR would limit the surgery. Therefore, analyses were also performed according to the T0 FLR. Patients with lower FLR may benefit the most from a sophisticated dosimetric study prior to SIRT, in order to tailor the activity to administer for an expected dose to the tumoral volume with intention to treat, and to the NTL volume, to produce hypertrophy of the non-treated liver, along with an increase in the FLR to 30–40% [36].

Conclusions

To our knowledge, this is the first study to investigate dosimetric parameters of ^{90}Y PET/CT that may predict atrophy of the treated liver segments and contralateral hypertrophy. Variables related to the dose absorbed by the NTL (mean dose and the fraction of the non-tumoral-treated volume exposed to at least 30 Gy, V30) were significantly predictive of hypertrophy and increase in FLR, particularly among patients in whom baseline FLR was < 30%. When half of NTL received ≥ 30 Gy, FLR increased to ≥ 40%, with higher accuracy among patients with FLR < 30% at T0. Hypertrophy and increase in FLR were not significantly associated with any dosimetric variables related to tumor dose or tumor size.

Supplementary Information The online version contains supplementary material available at https://doi.org/10.1007/s00259-021-05272-9.

Acknowledgements The authors gratefully acknowledge the effort and the excellent technical support of the Cyclotron and PET/CT staff.

Code availability PET-based voxel dosimetry was performed using a dedicated treatment planning system (PLANET Dose; DOSIsoft SA).

Funding This research did not receive any specific grant from funding agencies in the public, commercial, or not-for-profit sectors.

Data availability The datasets generated during and/or analyzed during the current study are available from the corresponding author on reasonable request.

Declarations

Ethics approval The institutional ethics committee approved the protocol (212/2019) for this retrospective study. Informed consent was waived.

Consent to participate NA.

Consent for publication NA.

Conflict of interest M.R.-F. and M.I. are paid speakers for Sirtex Medical Europe GmbH. B.S. is a paid consultant and speaker for Sirtex Medical and BTG. The authors declare no conflicts of interest.

References

1. Braat AJAT, Smits MLJ, Braat MNGJA, van den Hoven AF, Prince JF, de Jong HWAM, et al. 90Y hepatic radioembolization: an update on current practice and recent developments. J Nucl Med. 2015;56:1079–87.
2. Sangro B, Gil-Alzugaray B, Rodriguez J, Sola I, Martinez-Cuesta A, Viudez A, et al. Liver disease induced by radioembolization of liver tumors: description and possible risk factors. Cancer. 2008;112:1538–46.
3. Seidensticker M, Burak M, Kalinski T, Garlipp B, Koelble K, Wust P, et al. Radiation-induced liver damage: correlation of histopathology with hepatobiliary magnetic resonance imaging, a feasibility study. Cardiovasc Intervent Radiol. 2015;38:213–21.
4. Kim RD, Kim JS, Watanabe G, Mohuczy D, Behrns KE. Liver regeneration and the atrophy-hypertrophy complex. Semin Intervent Radiol Thieme Medical Publishers. 2008;25:92–103.
5. Jakobs TF, Saleem S, Atassi B, Reda E, Lewandowski RJ, Yaghmai V, et al. Fibrosis, portal hypertension, and hepatic volume changes induced by intra-arterial radiotherapy with90Yttrium microspheres. Dig Dis Sci. 2008;53:2556–63.
6. Gaba RC, Lewandowski RJ, Kulik LM, Riaz A, Ibrahim SM, Mulcahy MF, et al. Radiation lobectomy: preliminary findings of hepatic volumetric response to lobar yttrium-90 radioembolization. Ann Surg Oncol. 2009;16:1587–96.
7. Vouche M, Lewandowski RJ, Atassi R, Memon K, Gates VL, Ryu RK, et al. Radiation lobectomy: time-dependent analysis of future liver remnant volume in unresectable liver cancer as a bridge to resection. J Hepatol European Association for the Study of the Liver. 2013;59:1029–36.
8. Edeline J, Lenoir L, Boudjema K, Rolland Y, Boulic A, Le Du F, et al. Volumetric changes after 90Y radioembolization for hepatocellular carcinoma in cirrhosis: an option to portal vein embolization in a preoperative setting? Ann Surg Oncol. 2013;20:2518–25.
9. Ahmadzadehfar H, Meyer C, Ezziddin S, Sabet A, Hoff-Meyer A, Muckle M, et al. Hepatic volume changes induced by radioembolization with 90Y resin microspheres. A single-centre study. Eur J Nucl Med Mol Imaging. 2013;40:80–90.

10. Garlipp B, de Baere T, Damm R, Irmscher R, van Buskirk M, Stübs P, et al. Left-liver hypertrophy after therapeutic right-liver radioembolization is substantial but less than after portal vein embolization. Hepatology John Wiley and Sons Ltd. 2014;59:1864–73.
11. Teo JY, Goh BKP, Cheah FK, Allen JC, Lo RHG, Ng DCE, et al. Underlying liver disease influences volumetric changes in the spared hemiliver after selective internal radiation therapy with 90Y in patients with hepatocellular carcinoma. J Dig Dis Blackwell Publishing. 2014;15:444–50.
12. Teo JY, Allen JC, Ng DC, Choo SP, Tai DWM, Chang JPE, et al. A systematic review of contralateral liver lobe hypertrophy after unilobar selective internal radiation therapy with Y90. Hpb. International Hepato-Pancreato-Biliary Association Inc. 2016;18:7–12.
13. Fernández-Ros N, Silva N, Bilbao JI, Iñarrairaegui M, Benito A, D'Avola D, et al. Partial liver volume radioembolization induces hypertrophy in the spared hemiliver and no major signs of portal hypertension. HPB. 2014;16:243–9.
14. Goh BKP. Measured versus estimated total liver volume to preoperatively assess the adequacy of future liver remnant. Ann Surg. 2015;262:e72.
15. Tanaka K, Shimada H, Matsuo K, Ueda M, Endo I, Togo S. Remnant liver regeneration after two-stage hepatectomy for multiple bilobar colorectal metastases. Eur J Surg Oncol. 2007;33:329–35.
16. Hemming AW, Reed AI, Howard RJ, Fujita S, Hochwald SN, Caridi JG, et al. Preoperative portal vein embolization for extended hepatectomy. Ann Surg. 2003;237:686–91discussion 691-3.
17. Lassmann M, Eberlein U. The relevance of dosimetry in precision medicine. J Nucl Med. 2018;59:1494–9.
18. Chiesa C, Maccauro M, Romito R, Spreafico C, Pellizzari S, Negri A, et al. Need, feasibility and convenience of dosimetric treatment planning in liver selective internal radiation therapy with (90)Y microspheres: the experience of the National Tumor Institute of Milan. Q J Nucl Med Mol Imaging. 2011;55:168–97.
19. Lam MGEH, Goris ML, Iagaru AH, Mittra ES, Louie JD, Sze DY. Prognostic utility of 90Y radioembolization dosimetry based on fusion 99mTc-macroaggregated albumin-99mTc-sulfur colloid SPECT. J Nucl Med. 2013;54:2055–61.
20. Tong AKT, Kao YH, Too C, Chin KFW, Ng DCE, Chow PKH. Yttrium-90 hepatic radioembolization: clinical review and current techniques in interventional radiology and personalized dosimetry. Br J Radiol. 2016;89.
21. Garin E, Lenoir L, Rolland Y, Edeline J, Mesbah H, Laffont S, et al. Dosimetry based on 99mTc-macroaggregated albumin SPECT/CT accurately predicts tumor response and survival in hepatocellular carcinoma patients treated with 90Y-loaded glass microspheres: preliminary results. J Nucl Med. 2012;53:255–63.
22. Garin E, Rolland Y, Laffont S, Edeline J. Clinical impact of 99mTc-MAA SPECT/CT-based dosimetry in the radioembolization of liver malignancies with 90Y-loaded microspheres. Eur J Nucl Med Mol Imaging. 2016;43:559–75.
23. Palard X, Edeline J, Rolland Y, Le Sourd S, Pracht M, Laffont S, et al. Dosimetric parameters predicting contralateral liver hypertrophy after unilobar radioembolization of hepatocellular carcinoma. Eur J Nucl Med Mol Imaging. 2018;45:392–401.
24. Gil-Alzugaray B, Chopitea A, Iñarrairaegui M, Bilbao JI, Rodriguez-Fraile M, Rodriguez J, et al. Prognostic factors and prevention of radioembolization-induced liver disease. Hepatology Wiley-Blackwell. 2013;57:1078–87.
25. Sirtex Medical. SIR-Spheres® Y-90 resin microspheres activity chart [Internet]. 2020 [cited 2020 Oct 2]. Available from: https://www.sirtex.com/media/168731/activity-chart-apm-us-368-v1-0220.pdf
26. Martí-Climent JM, Prieto E, Elosúa C, Rodríguez-Fraile M, Domínguez-Prado I, Vigil C, et al. PET optimization for improved assessment and accurate quantification of 90Y-microsphere biodistribution after radioembolization. Med Phys. John Wiley and Sons Ltd. 2014;41:092503.
27. Peterson JL, Vallow LA, Johnson DW, Heckman MG, Diehl NN, Smith AA, et al. Complications after 90Y microsphere radioembolization for unresectable hepatic tumors: an evaluation of 112 patients. Brachytherapy Elsevier. 2013;12:573–9.
28. Therasse P, Arbuck SG, Eisenhauer EA, Wanders J, Kaplan RS, Rubinstein L, et al. New guidelines to evaluate the response to treatment in solid tumors. J Natl Cancer Inst. 2000;92:205–16.
29. Guglielmi A, Ruzzenente A, Conci S, Valdegamberi A, Iacono C. How much remnant is enough in liver resection? Dig Surg. 2012;29:6–17.
30. Goebel J, Sulke M, Lazik-Palm A, Goebel T, Dechêne A, Bellendorf A, et al. Factors associated with contralateral liver hypertrophy after unilateral radioembolization for hepatocellular carcinoma. PLoS One. 2017;12:e0181488.
31. Alsultan AA, Braat AJAT, Smits MLJ, Barentsz MW, Bastiaannet R, Bruijnen RCG, et al. Current status and future direction of hepatic radioembolisation. Clin Oncol. 2020;33:106–16.
32. Pasciak AS, Bourgeois AC, Bradley YC. A microdosimetric analysis of absorbed dose to tumor as a function of number of microspheres per unit volume in 90Y Radioembolization. J Nucl Med. 2016;57:1020–6.
33. van Roekel C, Reinders MTM, van der Velden S, Lam MGEH, Braat MNGJA. Hepatobiliary imaging in liver-directed treatments. Semin Nucl Med. Elsevier Inc.; 2019;49:227–36.
34. Braat MNGJA, de Jong HW, Seinstra BA, Scholten M V., van den Bosch MAAJ, Lam MGEH. Hepatobiliary scintigraphy may improve radioembolization treatment planning in HCC patients. EJNMMI Res. EJNMMI Research; 2017;7.
35. Bilbao JI, De Martino A, De Luis E, Díaz-Dorronsoro L, Alonso-Burgos A, Martínez De La Cuesta A, et al. Biocompatibility, inflammatory response, and recannalization characteristics of nonradioactive resin microspheres: histological findings. Cardiovasc Intervent Radiol. 2009;32:727–36.
36. Liu H, Zhu S. Present status and future perspectives of preoperative portal vein embolization. Am J Surg Elsevier. 2009;197:686–90.

Terms and Conditions

Springer Nature journal content, brought to you courtesy of Springer Nature Customer Service Center GmbH (“Springer Nature”).
Springer Nature supports a reasonable amount of sharing of research papers by authors, subscribers and authorised users (“Users”), for small-scale personal, non-commercial use provided that all copyright, trade and service marks and other proprietary notices are maintained. By accessing, sharing, receiving or otherwise using the Springer Nature journal content you agree to these terms of use (“Terms”). For these purposes, Springer Nature considers academic use (by researchers and students) to be non-commercial.
These Terms are supplementary and will apply in addition to any applicable website terms and conditions, a relevant site licence or a personal subscription. These Terms will prevail over any conflict or ambiguity with regards to the relevant terms, a site licence or a personal subscription (to the extent of the conflict or ambiguity only). For Creative Commons-licensed articles, the terms of the Creative Commons license used will apply.
We collect and use personal data to provide access to the Springer Nature journal content. We may also use these personal data internally within ResearchGate and Springer Nature and as agreed share it, in an anonymised way, for purposes of tracking, analysis and reporting. We will not otherwise disclose your personal data outside the ResearchGate or the Springer Nature group of companies unless we have your permission as detailed in the Privacy Policy.
While Users may use the Springer Nature journal content for small scale, personal non-commercial use, it is important to note that Users may not:

1. use such content for the purpose of providing other users with access on a regular or large scale basis or as a means to circumvent access control;
2. use such content where to do so would be considered a criminal or statutory offence in any jurisdiction, or gives rise to civil liability, or is otherwise unlawful;
3. falsely or misleadingly imply or suggest endorsement, approval , sponsorship, or association unless explicitly agreed to by Springer Nature in writing;
4. use bots or other automated methods to access the content or redirect messages
5. override any security feature or exclusionary protocol; or
6. share the content in order to create substitute for Springer Nature products or services or a systematic database of Springer Nature journal content.

In line with the restriction against commercial use, Springer Nature does not permit the creation of a product or service that creates revenue, royalties, rent or income from our content or its inclusion as part of a paid for service or for other commercial gain. Springer Nature journal content cannot be used for inter-library loans and librarians may not upload Springer Nature journal content on a large scale into their, or any other, institutional repository.
These terms of use are reviewed regularly and may be amended at any time. Springer Nature is not obligated to publish any information or content on this website and may remove it or features or functionality at our sole discretion, at any time with or without notice. Springer Nature may revoke this licence to you at any time and remove access to any copies of the Springer Nature journal content which have been saved.
To the fullest extent permitted by law, Springer Nature makes no warranties, representations or guarantees to Users, either express or implied with respect to the Springer nature journal content and all parties disclaim and waive any implied warranties or warranties imposed by law, including merchantability or fitness for any particular purpose.
Please note that these rights do not automatically extend to content, data or other material published by Springer Nature that may be licensed from third parties.
If you would like to use or distribute our Springer Nature journal content to a wider audience or on a regular basis or in any other manner not expressly permitted by these Terms, please contact Springer Nature at

onlineservice@springernature.com